Band gap and modal interaction analysis of metastructures with high-static-low-dynamic stiffness with multiple scales

Diego P. Vasconcellos[1], Marcos Silveira[1]

[1]*São Paulo State University (Unesp), School of Engineering.*
Av. Eng. Luiz Edmundo C. Coube 14-01-Vargem Limpa, 17033-360, São Paulo/Bauru, Brazil
diego.vasconcellos@unesp.br, marcos.silveira@unesp.br

Abstract. In this work, we explore the dynamical response of metastructures with high-static-low-dynamic stiffness (HSLDS) characteristics, with focus on the vibration attenuation performance through band gaps and band stops. A metastructure consists fundamentally of identical components, the cells, connected in a way that characteristics of mass, stiffness, and or damping are spatially repeated. Metastructures present interesting characteristics for vibration attenuation that are not found in classical structures. These characteristics have been explored for automotive and aerospace applications, among others, as structures with low mass are paramount for these industries, and keeping low vibration levels in a wide frequency range is also desirable. One unit cell with three degrees of freedom is used, with an axial harmonic force applied at the rightmost element. The dynamical response of the linear metastructure is found by mechanical impedance and transmissibility methods. The cell dynamical response of the nonlinear metastructure is found using the method of multiple scales (MMS), and the response is compared to the fourth-order Runge-Kutta method (RK). The influence of the mass ratio between the elements of the cell and number of cells in the complete structure are analysed in the frequency response of the metastructure.

Keywords: HSLDS, Metastructure, Vibration isolation, Multiple scales.

1 Introduction

Research on metastructures is attracting increasing attention from many engineering applications, such as civil, automotive and aerospace structures, as they have interesting characteristics such as band gaps and band stops [1]. These characteristics can be manipulated by the macro geometrical arrangement of its fundamental components, or unit cells, in a way that characteristics of mass, stiffness and or damping are spatially repeated and the resulting band gaps are in a desired frequency range [2–4]. According to Chakraborty and Mallik [5] an advantage of metastructure is that the dynamics of these structures can be studied with the analysis of just one cell. According to Mead [6] the limiting values of band gaps and band stops can be found by analyzing the natural frequencies of free and fixed cells, these frequency ranges can also be found by analyzing the transmissibility of a single cell [7].

In order to increase the bandwidth of vibration attenuation in metastructures, nonlinear characteristics have been explored in different ways. Both nonlinear stiffness and damping can affect the dynamic behavior of such structures [5, 8]. High-static-low-dynamic stiffness (HSLDS) is an example of nonlinearity and can be used to attenuate vibrations, as is done in [9] and [10]. The propagation of acoustic waves can also change due to nonlinear effects [11], besides that, metastructures with nonlinear characteristics can have chaotic responses in addition to the periodic ones more commonly observed [12].

To solve systems with nonlinearities it is possible to use the method of multiple scales (MMS), as exemplified by Nayfeh and Mook [13]. Some papers use the method of multiple scales, such as El-Bassiouny and Eissa [14] which analyzes a system with three degrees of freedom with cubic nonlinearity, El-Sayed and Bauomy [15] uses MMS to find approximate solutions for a nonlinear system with torsional vibration, to apply active and passive control methods to attenuate vibrations and Navazi and Hojjati [16] which uses MMS to analyze vibrations of an unbalanced rotor mounted on HSLDS supports. It is also possible to solve the nonlinear system using numerical methods, such as Vasconcellos and Silveira [17] which uses the Runge-Kutta method to analyze a metastructure with nonlinear stiffness.

In this work, we explore the performance of the metastructure for attenuation of axial vibration through the analysis of band gaps and band stops. The methods of mechanical impedance and transmissibility are used to define the limiting values of these frequency ranges, in addition to analyzing the influence of the mass ratio. And as it is seen that the nonlinearity can help in the attenuation of vibrations, the method of multiple scales is used to solve the cell of the metastructure with HSLDS and these results are compared with the fourth-order Runge-Kutta method.

2 Mathematical model

Figure 1 shows the model of metastructure with axial vibration $F(t)$ that are analyzed in this work, the dashed line shows one cell of this metastructure, the metastructure has mass, damping and stiffness coefficients named m_1 and m_2, c and k, respectively. In addition to HSLDS stiffness k_a, which has a geometric nonlinear behavior with influence on the displacement of the metastructure in x direction, and when it comes to the linear metastructure we have $k_a = 0$. The mass m_2 is written as a ratio of the mass m_1, as follows $m_2 = \mu m_1$, in which μ is the mass ratio.

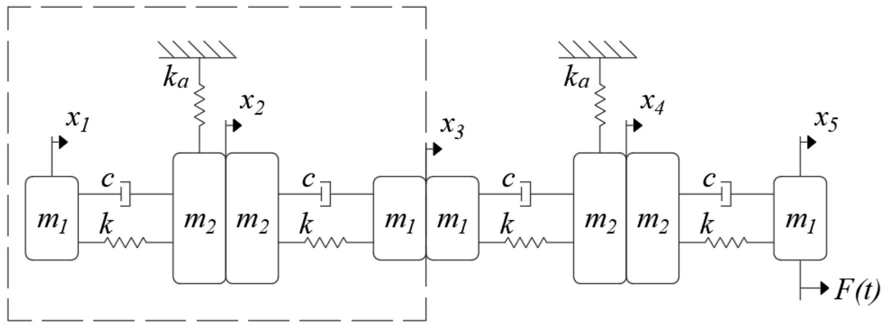

Figure 1. Schematic model of nonlinear metastructure.

The dynamical equations can be obtained by applying Newton's second law, giving the general form:

$$M\ddot{x} + C\dot{x} + Kx + G(x) = F(t) \tag{1}$$

in which M, C and K are the mass, damping and stiffness matrices, x is the displacement vector and $G(x)$ is a vector with nonlinear terms. $F(t)$ is the external force applied to the structure ($F(t) = F_0 \cos(\Omega t)$), in which F_0 is the amplitude and Ω is the frequency of excitation, and only the last element is nonzero. For the cell, the displacement vector is $x = [x_1, x_2, x_3]'$, and the matrices are given by eq. (2):

$$M = \begin{bmatrix} m_1 & 0 & 0 \\ 0 & 2\mu m_1 & 0 \\ 0 & 0 & m_1 \end{bmatrix} \quad C = \begin{bmatrix} c & -c & 0 \\ -c & 2c & -c \\ 0 & -c & c \end{bmatrix} K = \begin{bmatrix} k & -k & 0 \\ -k & 2k & -k \\ 0 & -k & k \end{bmatrix} \quad G(x) = \begin{bmatrix} 0 \\ \frac{k_a x_2^3}{2L_0^2} \\ 0 \end{bmatrix} \tag{2}$$

To solve the linear system, two methods are used, the method of mechanical impedance and the method of transmissibility, and for the nonlinear system, it is used the method of multiple scales.

For all three methods, it is important to define the natural frequencies of the cell, they can be found by defining the dynamic matrix as $A = M^{-1}K$, naming the natural frequencies as $\omega_{1,2,3}$, and defining $\lambda = \omega_{1,2,3}^2$, in which λ are the eigenvalues of A, and then it is possible to obtain the natural frequencies of the cell, as shown in eq. (3):

$$\omega_1 = 0 \qquad \omega_2 = \sqrt{\frac{k_1}{m_1}} \qquad \omega_3 = \sqrt{\frac{\mu k + k}{\mu m_1}} \tag{3}$$

3 Dynamical response of linear metastructure

First, the method of mechanical impedance is used to analyze the linear metastructure, in which the mechanical impedance Z is found by the following equation: $Z(i\Omega) = -\Omega^2 M + i\Omega C + K$. And the frequency response is found by solving X from the following equation: $X = [Z(i\Omega)]^{-1}F(t)$. Band gaps appear when the mass ratio is greater or less than 1, so the analysis of band gaps is done in two steps, the first is considering $\mu < 1$ and the second $\mu > 1$.

To identify the beginning and end of the band gap and band stop the natural frequencies shown in eq. (3) are used, in addition, it is necessary to find the natural frequencies when the cell is fixed in one of the ends, that is, when either the leftmost mass or the rightmost mass is fixed. To simulate the fixed cell, the first rows and columns of the matrices shown in equation (2) should be considered as zero to crimp the leftmost mass of the cell. Natural frequencies are given by:

$$\omega_{21} = \sqrt{-\frac{k\sqrt{\mu^2+1} - \mu k - k}{2\mu m_1}} \qquad \omega_{22} = \sqrt{\frac{k\sqrt{\mu^2+1} + \mu k + k}{2\mu m_1}} \tag{4}$$

The following nomenclature is used to identify the band gap and band stop, ω_a the beginning of the band gap, ω_b the end of the band gap and ω_c the band stop.

Figure 2 shows the frequency response of the leftmost mass (X_1), considering the metastructure with up to five cells ($n = 5$), as well as the natural frequencies and the frequency response of the fixed cell. The dashed line shows the value of 10^0, when the frequency response curve passes below this line, it is possible to identify where are the band gap and band stop limiters.

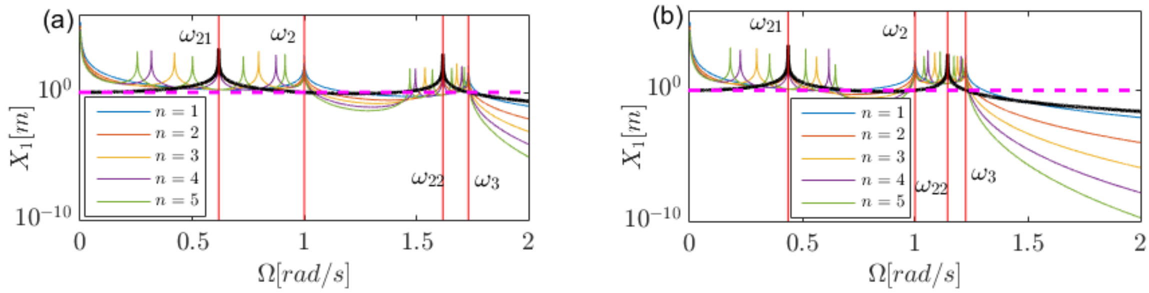

Figure 2. Frequency response with (a) $\mu < 1$ and (b) $\mu > 1$ for $n = 1, ..., 5$, fixed cell and the vertical lines indicating the natural frequencies.

From Fig. 2 (a) it is possible to identify the band gap and band stop for $\mu < 1$. The beginning of the band gap ω_a as being ω_2, the band stop ω_c as being ω_3 and the end of the band gap is split in two values, ω_{bl} and ω_{bu}, as it is depend on the number of cells in the metastructure, in which $\omega_{bu} = \omega_{22}$ and ω_{bl} is the n^{th} natural frequency of the metastructure, where n is the number of cells.

From Fig. 2 (b) it is possible to identify the band gap and band stop for $\mu > 1$. The end of the band gap ω_b as being ω_2, the band stop ω_c as being ω_3 and the beginning of the band gap is be split in two values ω_{al} and ω_{au}, as it is depend on the number of cells in the metastructure, where $\omega_{al} = \omega_{21}$ and ω_{au} is the n^{th-1} natural frequency of the metastructure.

And now the transmissibility (Tr) is used, which is basically a ratio between the response of the leftmost mass and the rightmost mass ($Tr = X_1/X_{2n+1}$). And to find the frequencies referring to the band gap and the band stop, must find the expressions to $|Tr| = 1$, these equations are shown in eq. (5). Note that ω_{2Tr} and ω_{3Tr}, are equal to ω_2 and ω_3 shown in eq. (3), respectively.

$$\omega_{1Tr} = \sqrt{\frac{k}{\mu m_1}} \qquad \omega_{2Tr} = \sqrt{\frac{k_1}{m_1}} \qquad \omega_{3Tr} = \sqrt{\frac{\mu k + k}{\mu m_1}} \tag{5}$$

Figure 3 shows the transmissibility for $\mu = 0.5$ and $\mu = 2$, with the vertical lines indicating the frequencies shown in eq. (5). It is possible to identify the band stop ω_c as ω_{3Tr} for both $\mu = 0.5$ and $\mu = 2$. For $\mu = 0.5$, the beginning of band gap is ω_{2Tr} and the end of band gap is ω_{1Tr}, and for $\mu = 2$, the beginning of band gap is ω_{1Tr} and the end of band gap is ω_{2Tr}.

4 Dynamical response of cell with HSLDS

The method of multiple scales is used to solve the problem of the cell with HSLDS, and to start the method it is necessary to decouple the system variables that are shown in eq. (1) and the matrices shown in eq. (2). To

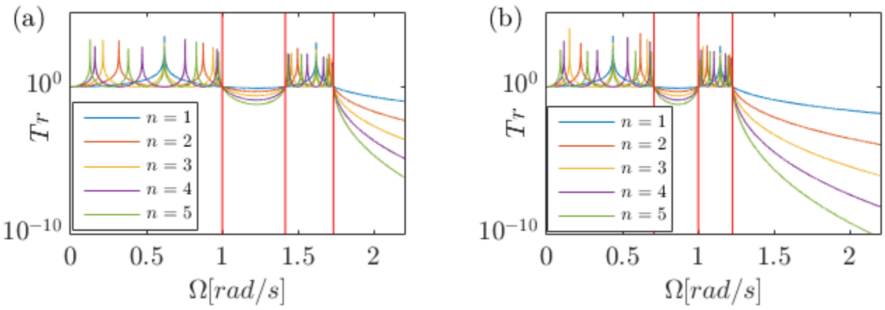

Figure 3. Transmissibility curve, where the vertical lines indicate the frequencies shown in eq. (5) (a) $\mu = 0.5$ and (b) $\mu = 2$

start the decoupling of the variables it is necessary to find the modal matrix Φ, where the columns of Φ are the eigenvalues of the dynamic matrix $A = M^{-1}K$. And the system is rewritten in function of the new coordinates η, following eq. (6):

$$\Phi^T M\Phi\ddot{\eta} + \Phi^T C\Phi\dot{\eta} + \Phi^T K\Phi\eta + \Phi^T G(x) - \Phi^T F = 0 \tag{6}$$

To write the nonlinear vector as a function of η it is necessary to make the coordinate transformation $X = \Phi\eta$, in which $x_1 = \eta_1 + \eta_2 + \eta_3$, $x_2 = \eta_1 - \frac{\eta_3}{\mu}$ and $x_3 = \eta_1 - \eta_2 + \eta_3$.

To solve eq. (8), the following expansion is used, where $j = 1, 2, 3$:

$$\eta_j = \epsilon\eta_{j1}(T_0, T_2) + \epsilon^3\eta_{j3}(T_0, T_2) \tag{7}$$

The terms $O(\epsilon^2)$ and T_1 are not used, as the nonlinearity effect appears in $O(\epsilon^3)$. In addition, the damping terms d_j are multiplied by ϵ^2 and the force terms f_j are multiplied by ϵ^3, so that the effect of damping, nonlinearity and excitation appears in the same perturbation equations.

$$\begin{aligned}
\ddot{\eta}_1 &= \alpha_1\eta_1^3 + \alpha_2\eta_1^2\eta_3 + \alpha_3\eta_1\eta_3^2 + \alpha_4\eta_3^3 + \epsilon^3 f_1\cos(\Omega t)\\
\ddot{\eta}_2 + \omega_2^2\eta_2 &= -\epsilon^2 d_2\dot{\eta}_2 + \epsilon^3 f_2\cos(\Omega t)\\
\ddot{\eta}_3 + \omega_3^2\eta_3 &= -\epsilon^2 d_3\dot{\eta}_3 + \alpha_5\eta_1^3 + \alpha_6\eta_1^2\eta_3 + \alpha_7\eta_1\eta_3^2 + \alpha_8\eta_3^3 + \epsilon^3 f_3\cos(\Omega t)
\end{aligned} \tag{8}$$

In which,

$$\begin{aligned}
&\alpha_1 = \frac{k_a}{2L_0^2(2\mu m_1 + 2m_1)},\quad \alpha_2 = -\frac{3k_a}{2L_0^2\mu(2\mu m_1 + 2m_1)},\quad \alpha_3 = \frac{3k_a}{2L_0^2\mu^2(2\mu m_1 + 2m_1)},\\
&\alpha_4 = -\frac{k_a}{2L_0^2\mu^3(2\mu m_1 + 2m_1)},\quad f_1 = \frac{F_0}{2\mu m_1 + 2m_1},\quad d_2 = \frac{c}{m_1},\quad \omega_2^2 = \frac{k}{m_1},\quad f_2 = -\frac{F_0}{2m_1},\\
&d_3 = \frac{2c\mu^2 + 4c\mu + 2c}{\mu(2\mu m_1 + 2m_1)},\quad \omega_3^2 = \frac{\mu k + k}{\mu m_1},\quad \alpha_5 = -\frac{k_a}{2L_0^2(2\mu m_1 + 2m_1)},\quad \alpha_6 = \frac{3k_a}{2L_0^2\mu(2\mu m_1 + 2m_1)}\\
&\alpha_7 = -\frac{3k_a}{2L_0^2\mu^2(2\mu m_1 + 2m_1)},\quad \alpha_8 = \frac{k_a}{2L_0^2\mu^3(2\mu m_1 + 2m_1)},\quad f_3 = \frac{\mu F_0}{2\mu m_1 + 2m_1}
\end{aligned} \tag{9}$$

Substituting 7 into 8 and equating the coefficients ϵ and ϵ^3 to zero, we obtain to order ϵ eq. (10) and to order ϵ^3 eq. (11).

$$D_0^2\eta_{11} = 0 \qquad D_0^2\eta_{21} + \omega_2^2\eta_{21} = 0 \qquad D_0^2\eta_{31} + \omega_2^2\eta_{31} = 0 \tag{10}$$

$$\begin{aligned}
D_0^2\eta_{13} + 2D_0D_2\eta_{11} - \alpha_1\eta_{11}^3 - \alpha_2\eta_{11}^2\eta_{31} - \alpha_3\eta_{11}\eta_{31}^2 - \alpha_4\eta_{31}^3 - f_1\cos(\Omega t) = 0\\
D_0^2\eta_{23} + \omega_2^2\eta_{23} + 2D_0D_2\eta_{21} + D_0d_2\eta_{21} - f_2\cos(\Omega t) = 0\\
D_0^2\eta_{33} + \omega_3^2\eta_{33} + 2D_0D_2\eta_{31} + D_0d_3\eta_{31} - \alpha_5\eta_{11}^3 - \alpha_6\eta_{11}^2\eta_{31} - \alpha_7\eta_{11}\eta_{31}^2 - \alpha_8\eta_{31}^3 - f_3\cos(\Omega t) = 0
\end{aligned} \tag{11}$$

Remembering that $D_n = \partial/\partial T_n$. And solving eq. (10) in exponential form, we obtain:

$$\eta_{11} = k_1 + k_2 T_0 \qquad \eta_{21} = A_2(T_2)e^{i\omega_2 T_0} + cc \qquad \eta_{31} = A_3(T_2)e^{i\omega_3 T_0} + cc \tag{12}$$

Considering $k_1 = k_2 = 0$ and replacing eq. (12) in eq. (11), we obtain the following equations:

$$\begin{aligned} D_0^2\eta_{13} &= A_3^3\alpha_4 e^{3iT_0\omega_3} + 3A_3^2\bar{A}_3\alpha_4 e^{iT_0\omega_3} + \frac{f_1}{2}e^{i\Omega T_0} + cc \\ \eta_{23}\omega_2^2 + D_0^2\eta_{23} &= -D_0(A_2 d_2 + 2A_2 D_2)e^{iT_0\omega_2} + \frac{f_2}{2}e^{i\Omega T_0} + cc \\ \eta_{33}\omega_3^2 + D_0^2\eta_{33} &= A_3^3\alpha_8 e^{3iT_0\omega_3} - D_0(A_3 d_3 + 2A_3 D_2)e^{iT_0\omega_3} + 3A_3^2\bar{A}_3\alpha_8 e^{iT_0\omega_3} + \frac{f_3}{2}e^{i\Omega T_0} + cc \end{aligned} \tag{13}$$

where cc stands for the complex conjugate of the preceding terms. In next two subsections, two resonant cases of the nonlinear cell are analyzed, the case in which $\Omega \approx \omega_2$ and the case of $\Omega \approx \omega_3$.

The case of Ω near ω_2

To measure the nearness of Ω with ω_2, the detuning parameter σ_2 is introduced, according to: $\Omega = \omega_2 + \epsilon^2\sigma_2$. To remove the secular terms from η_{j3}, the terms proportional to $e^{i\omega_{1,2,3}T_0}$ must disappear. Secular terms are shown in eq. (14), in which there are no terms proportional to $e^{i\omega_1 T_0}$, since, as already shown, $\omega_1 = 0$.

$$A_2 D_0 d_2 + 2A_2 D_0 D_2 - \frac{f_2}{2}e^{i\sigma_2 T_2} = 0 \qquad A_3 D_0 d_3 + 3A_3^2\bar{A}_3\alpha_8 + 2A_3 D_0 D_2 = 0 \tag{14}$$

Where $D_0 = i\omega_{1,2,3}$, writing A_m in polar notation $A_m = \frac{1}{2}a_m e^{i\theta_m}$, with a_m and θ_m being real numbers. Separating into real and imaginary parts, and considering an autonomous system with $\gamma_2 = \sigma_2 T_2 - \theta_2$, we have the modulation equations:

$$\frac{a_2\omega_2 d_2}{2} + a_2'\omega_2 - \frac{f_2\sin(\gamma_2)}{2} = 0 \qquad \frac{a_3 d_3\omega_3}{2} + a_3'\omega_3 = 0 \tag{15}$$

$$a_2\omega_2\sigma_2 - a_2\omega_2\gamma_2' + \frac{f_2\cos(\gamma_2)}{2} = 0 \qquad a_3\omega_3\theta_3' + \frac{3a_3^3\alpha_8}{8} = 0 \tag{16}$$

The steady-state solution of the modulation equations can be obtained by setting derivatives equal zero, with this we obtain $a_3 = 0$. By squaring and summing the remaining equations, it is possible to find a relationship between a_2 and σ_2, as shown in eq. (17).

$$\sigma_2 = \pm\frac{\sqrt{f_2 - a_2^2 d_2^2\omega_2^2}}{2a_2\omega_2} \tag{17}$$

Equation (17) can be used to show the amplitude of motion as a function of excitation frequency, as shown in Fig. 4. Nominal parameters are: $\epsilon = 1$, $m_1 = 1$, $k = 1$, $L_0 = 1$, $c = 0.1$ and $F_0 = 1$. This figure also include a comparison between the response obtained with multiple scales and with Runge-Kutta methods.

The case of Ω near ω_3

To measure the nearness of Ω with ω_3, the detuning parameter σ_3 is introduced, according to: $\Omega = \omega_3 + \epsilon^2\sigma_3$. To remove the secular terms from η_{j3}, the terms proportional to $e^{i\omega_{1,2,3}T_0}$ must disappear. Secular terms are shown in eq. (18), in which there are no terms proportional to $e^{i\omega_1 T_0}$, since, as already shown, $\omega_1 = 0$.

$$A_2 D_0 d_2 + 2A_2 D_0 D_2 = 0 \qquad A_3 D_0 d_3 - 3A_3^2\bar{A}_3\alpha_8 + 2A_3 D_0 D_2 - \frac{f_3}{2}e^{i\sigma_3 T_2} = 0 \tag{18}$$

Where $D_0 = i\omega_{1,2,3}$, and writing A_m in polar notation $A_m = \frac{1}{2}a_m e^{i\theta_m}$, with a_m and θ_m being real numbers. Separating into real and imaginary, and considering $\gamma_3 = \sigma_3 T_2 - \theta_3$, we have the modulation equations:

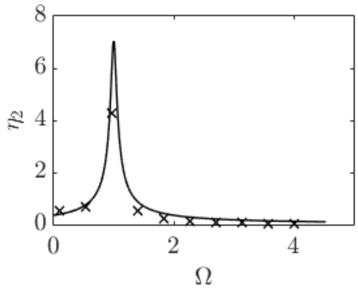

Figure 4. Displacement amplitude η_2 as function of excitation frequency Ω, with $\Omega \approx \omega_2$. Parameters: $\epsilon = 1$, $m_1 = 1$, $k = 1$, $L_0 = 1$, $c = 0.1$ and $F_0 = 1$. Solid line are obtained with multiple scales, markers are obtained with Runge-Kutta.

$$\frac{a_2\omega_2 d_2}{2} + a_2'\omega_2 = 0 \qquad -\frac{a_3 d_3 \omega_3}{2} + a_3'\omega_3 - \frac{f_3\sin(\gamma_3)}{2} = 0 \tag{19}$$

$$a_2\omega_2\theta_2' = 0 \qquad a_3\omega_3\sigma_3 - a_3\omega_3\gamma_3' + \frac{3a_3^3\alpha_8}{8} + \frac{f_3\cos(\gamma_3)}{2} = 0 \tag{20}$$

The steady-state solution of the modulation equations can be obtained by setting derivatives equal zero, with this we obtain $a_2 = 0$. By squaring and summing the remaining equations, it is possible to find a relationship between a_3 and σ_3, as shown in eq. (21).

$$\sigma_3 = \pm\frac{\sqrt{f_3^2 - a_3^2 d_3^2 \omega_3^2}}{2a_3\omega_3} - \frac{3a_3^2\alpha_8}{8\omega_3} \tag{21}$$

Equation (21) can be used to show the amplitude of motion as a function of excitation frequency, as shown in Fig. 5. Nominal parameters are: $m_1 = 1$, $k = 1$, $L_0 = 1$, $c = 0.1$, $F_0 = 1$, $\epsilon = 1$, $\mu = 0.5$, $\mu = 1$, $\mu = 2$, $k_a = -100$, $k_a = 0$, $k_a = 100$. This figure also include a comparison between the response obtained with multiple scales and with Runge-Kutta methods.

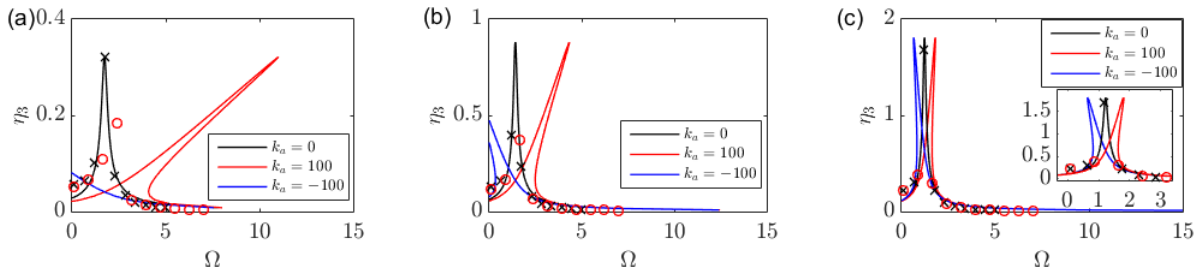

Figure 5. Displacement amplitude η_3 as function of excitation frequency Ω, with $\Omega \approx \omega_3$ in which (a) $\mu = 0.5$, (b) $\mu = 1$ and (c) $\mu = 2$. Parameters: $m_1 = 1$, $k = 1$, $L_0 = 1$, $c = 0.1$, $F_0 = 1$, $\epsilon = 1$, $k_a = -100$ (softening), $k_a = 0$, $k_a = 100$ (hardening). Solid line are obtained with multiple scales, markers are obtained with Runge-Kutta.

5 Conclusions

In this work, we explore the performance of the metastructure for attenuation of axial vibration through the analysis of band gaps and band stops. From the results shown using the methods of mechanical impedance and transmissibility, we can show that it is possible to find the limiting values of band gaps and band stops by analyzing the natural frequencies of a single cell with free and fixed boundary conditions, and to confirm these values, metastructure results with up to five cells were shown. To analyze the metastructure with HSLDS was used the method of multiple scales. Were analyzed two resonant cases, the case in which the frequency of excitation Ω is near to ω_2 and the case in which Ω is near to ω_3, both resonant cases using the method of multiple scales were compared with results using the fourth-order Runge-Kutta method. It is possible to note that, for the linear metastructure $k_a = 0$, the MMS and RK responses are close, and for the nonlinear case $k_a = 100$, that is, hardening stiffness, the responses of the MMS and RK methods get closer as the value of the mass ratio μ is increased.

Acknowledgements. The first author thanks Coordenação de Aperfeiçoamento de Pessoal de Nível Superior – Brazil (CAPES), for the financial support (Finance Code # 88887.487915/2020-00). The second author thanks FAPESP # 2018/15894-0.

Authorship statement. The authors hereby confirm that they are the sole liable persons responsible for the authorship of this work, and that all material that has been herein included as part of the present paper is either the property (and authorship) of the authors, or has the permission of the owners to be included here.

References

[1] M. I. Hussein, M. J. Leamy, and M. Ruzzene. Dynamics of phononic materials and structures: Historical origins, recent progress, and future outlook. *Applied Mechanics Reviews*, vol. 66, n. 4, 2014.

[2] L. Cveticanin, M. Zukovic, and D. Cveticanin. Influence of nonlinear subunits on the resonance frequency band gaps of acoustic metamaterial. *Nonlinear Dynamics*, vol. 93, pp. 1–11, 2018.

[3] C. H. Lamarque, A. Ture Savadkoohi, and S. Charlemagne. Experimental results on the vibratory energy exchanges between a linear system and a chain of nonlinear oscillators. *Journal of Sound and Vibration*, vol. 437, pp. 97–109, 2018.

[4] D. M. Mead. Wave propagation in continuous periodic structures: research contributions from southampton, 1964–1995. *Journal of sound and vibration*, vol. 190, n. 3, pp. 495–524, 1996.

[5] G. Chakraborty and A. K. Mallik. Dynamics of a weakly non-linear periodic chain. *International Journal of Non-Linear Mechanics*, vol. 36, n. 2, pp. 375–389, 2001.

[6] D. J. Mead. Wave propagation and natural modes in periodic systems: I. mono-coupled systems. *Journal of Sound and Vibration*, vol. 40, n. 1, pp. 1–18, 1975.

[7] P. Gonçalves, M. Brennan, and V. Cleante. Predicting the stop-band behaviour of finite mono-coupled periodic structures from the transmissibility of a single element. *Mechanical Systems and Signal Processing*, vol. 154, pp. 107512, 2021.

[8] A. Marathe and A. Chatterjee. Wave attenuation in nonlinear periodic structures using harmonic balance and multiple scales. *Journal of Sound and Vibration*, vol. 289, n. 4-5, pp. 871–888, 2006.

[9] A. Carrella. *Passive vibration isolators with high-static-low-dynamic-stiffness*. PhD thesis, University of Southampton, 2008.

[10] A. Carrella, M. Brennan, T. Waters, and V. Lopes Jr. Force and displacement transmissibility of a nonlinear isolator with high-static-low-dynamic-stiffness. *International Journal of Mechanical Sciences*, vol. 55, n. 1, pp. 22–29, 2012.

[11] Y. Yun, G. Q. Miao, P. Zhang, K. Huang, and R. J. Wei. Nonlinear acoustic wave propagating in one-dimensional layered system. *Physics Letters A*, vol. 343, n. 5, pp. 351–358, 2005.

[12] A. F. Vakakis and M. E. King. Resonant oscillations of a weakly coupled, nonlinear layered system. *Acta mechanica*, vol. 128, n. 1-2, pp. 59–80, 1998.

[13] A. H. Nayfeh and D. T. Mook. *Nonlinear Oscillations*. Wiley Classics Library, 1995.

[14] A. El-Bassiouny and M. Eissa. Response of three-degree-of-freedom system with cubic non-linearities to harmonic excitations. *Physica Scripta*, vol. 59, n. 3, pp. 183, 1999.

[15] A. T. El-Sayed and H. S. Bauomy. Passive and active controllers for suppressing the torsional vibration of multiple-degree-of-freedom system. *Journal of Vibration and Control*, vol. 21, n. 13, pp. 2616–2632, 2015.

[16] H. Navazi and M. Hojjati. Nonlinear vibrations and stability analysis of a rotor on high-static-low-dynamic-stiffness supports using method of multiple scales. *Aerospace Science and technology*, vol. 63, pp. 259–265, 2017.

[17] D. P. Vasconcellos and M. Silveira. Optimization of axial vibration attenuation of periodic structure with nonlinear stiffness without addition of mass. *Journal of Vibration and Acoustics*, vol. 142, n. 6, pp. 061009, 2020.